




Cite this: *RSC Adv.*, 2022, 12, 8485

Microfluidic fluorescent platform for rapid and visual detection of veterinary drugs†

Ge Li, Hao Li, Jiang Zhai, Jiazhuang Guo, Qing Li, Cai-Feng Wang * and Su Chen 

The overuse of veterinary drugs and veterinary drug residues is increasingly becoming an obstacle to sustainable development worldwide. It is therefore imperative to establish a quantitative, sensitive and efficient method for the detection of veterinary drugs. Herein, we developed a visual microfluidic detection platform for rapid and sensitive detection of veterinary drugs using CdTe quantum dots (QDs) with three different ligands as the sensing units. Green-emissive 3-mercaptopropionic acid (MPA)-CdTe QDs, yellow-emissive thioglycolic acid (TGA)-CdTe QDs and orange-emissive *N*-acetyl-L-cysteine (NAC)-CdTe QDs were synthesized by a sulfhydryl aqueous phase method. These CdTe QDs show selective rapid fluorescence response to pefloxacin (PEF), malachite green (MG), and 1-aminohydantoin hydrochloride (AHD). With the concentration of veterinary drugs increasing, the CdTe QDs reveals a fluorescence color variation from bright to dark until quenched and the response degree of CdTe QDs with different ligands to veterinary drugs is different. Specifically, the limits of detection (LODs) of MPA-CdTe, TGA-CdTe and NAC-CdTe QDs probes for PEF were 7.57 μ M, 1.75 μ M and 2.90 μ M, respectively, and the response was complete in a few seconds, realizing the sensitive and rapid detection of PEF. The three kinds of CdTe QDs could also be used in the detection of other veterinary drugs such as MG and AHD. Finally, a microfluidic detection platform was constructed for visual sensing and rapid detection towards veterinary drugs. The sensor platform holds the advantages of simple operation, low cost, rapid sensing and good sensitivity, and is potentially useful for visual quantitative detection of veterinary drug residues in aquatic products and the environment.

Received 29th January 2022
Accepted 11th March 2022

DOI: 10.1039/d2ra00626j

rsc.li/rsc-advances

Introduction

Veterinary drugs are widely used in modern agriculture and animal husbandry to prevent the devastating losses of large-scale diseases, pests and epidemics.¹ However, the use of large amounts of veterinary drugs has brought about the problem of drug residues in environmental water and food.² These residues bring risks to human health, such as cancers, birth defects, or hormone disruption.^{3,4} Veterinary drug residues in environmental water and food are not only harmful to people's health, but also affect the export of agricultural and aquatic products.⁵ As there is a growing demand for environmental protection and food safety, many countries have promulgated various constraints and regulations to strictly limit veterinary drug residues in environmental water and food.

Currently, the detection methods for veterinary drug residues mainly contain instrumental analysis and immunoassay,⁶

including high performance liquid chromatography-ultraviolet detection (HPLC-UV),⁷ high performance liquid chromatography-fluorescence (HPLC-FL),⁸ high performance liquid chromatography-mass spectrometry (HPLC-MS),⁹ enzyme-linked immunosorbent assay (ELISA),^{10,11} high resolution mass spectrometry (HRMS)¹² and so on. Although instrumental analysis holds good accuracy and sensitivity, its high cost and complex operation steps deter people.¹³ The merits of immunoassay include simple sample processing, high specificity, low cost and simple operation, while the high false positive and poor repeatability become big problems.^{14,15} It is still of great practical significance to develop rapid, sensitive and efficient detection methods for veterinary drug residues.

With the rapid development of nano-science, quantum dots (QDs) have emerged as active fluorescent probes. Due to their unique optical characteristics, excellent photochemical stability, easy synthesis and rapid detection of target analytes, QDs are widely used in life science,¹⁶ environmental detection,¹⁷ biochemical sensing,¹⁸ bioimaging,¹⁹ immunoassay,²⁰ medical diagnosis²¹ and many other research fields.²² In recent years, QDs have attracted extensive attention and greatly promoted the development of fluorescence immunoassay.²³ In particular, it was found that QDs modified with different surface

State Key Laboratory of Materials-Oriented Chemical Engineering, College of Chemical Engineering, Jiangsu Key Laboratory of Fine Chemicals and Functional Polymer Materials, Nanjing Tech University, Nanjing 210009, China. E-mail: caifengwang@njtech.edu.cn; chensu@njtech.edu.cn; Tel: +86-25-83172258

† Electronic supplementary information (ESI) available. See DOI: 10.1039/d2ra00626j



functional groups exhibited photoluminescence or chemiluminescence response to external stimulation, indicating their excellent sensing potential.²⁴ Fluorescence correlation detection technology is becoming high-profile and also show prospects in the field of veterinary drug residue detection.^{25,26}

In this study, we constructed a simple microfluidic sensing system as a fluorescent probe platform, based on the optical properties of CdTe QDs with three different ligands, allowing the detection of veterinary drugs. Three kinds of CdTe QDs with good water solubility, high fluorescence intensity, uniform dispersion and narrow size distribution were synthesized by an aqueous phase method. CdTe QDs show a clear fluorescence intensity and color variation within a short time after mixing with veterinary drugs. A microfluidic chip was designed for the rapid detection of veterinary drugs using different colored CdTe QDs capped with different ligands as fluorescent probes. It is reusable, cost-saving and beneficial for environmental protection. Combined with the visualized microfluidic detection platform, a simple, rapid and intuitive method for the detection of veterinary drugs on samples can be implemented. Significantly, on this visualized microfluidic detection platform, CdTe QDs with different ligands could be used for the detection of different kinds of veterinary drugs such as pefloxacin (PEF), malachite green (MG), and 1-aminohydantoin hydrochloride (AHD), with sensitive detection effect, good correlation and low LOD. The probe showed sensitive response to PEF, MG and AHD, and was successfully applied to the detection of unknown concentrations of veterinary drugs. The response is rapid and visual owing to the reaction between surface functional groups of CdTe QDs and veterinary drugs molecules. More importantly, benefitting from the merits of microfluidic chip microchannels, the surface functional groups of CdTe QDs can fully react with veterinary drugs molecules, which further improves the reaction time and sensitivity. In addition, due to the advantages of visualization of the microfluidic device, the fluorescence intensity information can be captured in time. This sensor platform shows a broad application prospect in real-time quantitative detection of veterinary drug residues with rapid, sensitive and visual features, meaningful for food and environmental safety.

Experimental

Materials and reagents

Cadmium chloride hemi (pentahydrate) ($\text{CdCl}_2 \cdot 2.5\text{H}_2\text{O}$, 99%), 3-mercaptopropionic acid (MPA, 99%), thioglycolic acid (TGA, 99%) and *N*-acetyl-L-cysteine (NAC, 99%) were purchased from Tianjin Chemical Reagents Co. Ltd. Tellurium (Te) powder (99.99%), sodium borohydride (NaBH_4 , 99.5%) and sodium hydroxide (NaOH , $\geq 85\%$) were purchased from Sinopharm Chemical Reagents Co. Ltd. Pefloxacin (PEF, 99%), malachite green (MG, 99%), 1-aminohydantoin hydrochloride (AHD, 99%) and chloramphenicol (CAP, 99%) were purchased from Shanghai Macklin Biochemical Technology Co. Ltd. All chemicals were of analytical reagent grade and required no further purification prior to use. All solutions were prepared using ultrapure water with a resistivity of 18.2 m Ω , obtained from

Sinopharm Chemical Reagent Co. Ltd. Pure water was provided by Hangzhou Wahaha Group Co., Ltd, China.

Synthesis of NaHTe

NaHTe was prepared according to a method described previously in the literature,²⁷ with some modifications. Briefly, 0.5 mmol of Te powder and 3.0 mmol of NaBH_4 (1 : 6 molar ratio of Te to NaBH_4) were loaded into a 5 mL strain flask and 2 mL of pure water was added. The strain flask was sealed with a rubber stopper into which a small needle was inserted to allow the release of the hydrogen (H_2) gas produced by the reaction. After 8 hours of reaction in an ice bath, the bottom of the strain bottle formed white sodium tetraborate crystals and the black Te powder disappeared completely. The upper clarified layer was a lavender solution of NaHTe, which was used as a Te precursor in the subsequent preparation.

Synthesis of CdTe QDs with different ligands

The synthesis of CdTe QDs was performed according to a previously reported procedure.²⁷ In a typical synthesis, 1 mmol $\text{CdCl}_2 \cdot 2.5\text{H}_2\text{O}$ was weighed into a 100 mL three-necked flask with a condenser and 40 mL of pure water was added to dissolve it. Then 5 mL of aqueous solution containing organic ligand (2.5 mmol MPA or 0.5 mmol TGA or 1.5 mmol NAC) was injected under vigorous stirring. The pH value of the solution was adjusted to 9–10 with use of an aqueous solution of NaOH (5 M), introduced with nitrogen (N_2) gas and stirred for 30 minutes. After that, the solution was heated and kept at a constant temperature of 95 °C. The freshly prepared NaHTe solution was quickly injected into the above solution using a syringe. In order to obtain different sizes of CdTe QDs, the reaction mixture was taken in equal amounts at different intervals of time for PL spectra measurements. The solution obtained was precipitated with ethanol and centrifuged at 8000 rpm for 10 min. The resulting precipitate was washed with ethanol and then reprecipitated 3 times, dried under vacuum and stored in a sealed container away from light.

Fluorescence detection for veterinary drugs residues based on CdTe QDs with different ligands

Fresh aqueous solutions of MPA-CdTe, TGA-CdTe and NAC-CdTe QDs were prepared (1 mg mL⁻¹). Different concentrations of veterinary drug solutions were prepared. A series of known concentrations of veterinary drug solutions were added to the prepared CdTe QDs solutions, respectively, and the change of fluorescence intensity with the concentration of veterinary drug solution was measured by fluorescence spectrophotometer. According to the fluorescence intensity of the tested solution, a relationship between the fluorescence intensity and the concentration of the veterinary drug solution was established.



Detection for veterinary drugs *via* visual microfluidic detection platform

First, microfluidic chips were manufactured by carving 2 mm thick polymethyl methacrylate (PMMA) substrates with parameters as follows: inlet pipe diameter of 0.8 mm, serpentine pipe diameter of 1.6 mm, circular holes diameter of 4 mm, depth of circular holes of 1.6 mm, spacing distance of circular holes of 4 mm and buffer pool of 5×10 mm. Subsequently, a blotting paper with a diameter of 3 mm was placed into each circular hole of the detection chamber, and then the chip was covered with a detachable sealing layer. Then, CdTe QDs with different ligands (5 μ L) were separately injected into circular holes filled with blotting papers as fluorescent probes. Finally, the prepared microfluidic fluorescence detection chip was put into the microfluidic device and connected with the injection pump for subsequent veterinary drug detection. The solution containing unknown concentration of veterinary drugs was flowed into the chip through a simple microfluidic device. The sample solution was flowed through a serpentine micro-channel into the detection chamber, where different QDs were quenched to varying degrees. According to the linear relationship between fluorescence intensity and veterinary drug concentration, the veterinary drug concentration in the tested solution was determined.

Measurements

The microstructure of CdTe QDs was characterized by transmission electron microscopy (TEM) (FEI TECNAI G2 F20). X-ray diffraction (XRD) patterns were collected using a ARL X'TRA powders X-ray diffractometer. Fourier transform infrared (FT-IR) spectra were performed on a Nicolet 6700 FT-IR spectrophotometer. Ultraviolet-visible (UV-Vis) absorption spectra of the CdTe QDs were performed on a PerkinElmer Lambda 900 UV-Vis spectrophotometer. The PL spectra were performed on a Varian Cary Eclipse spectrophotometer. The lifetime decay curves of CdTe QDs were measured using an Edinburgh FLS 980-STM.

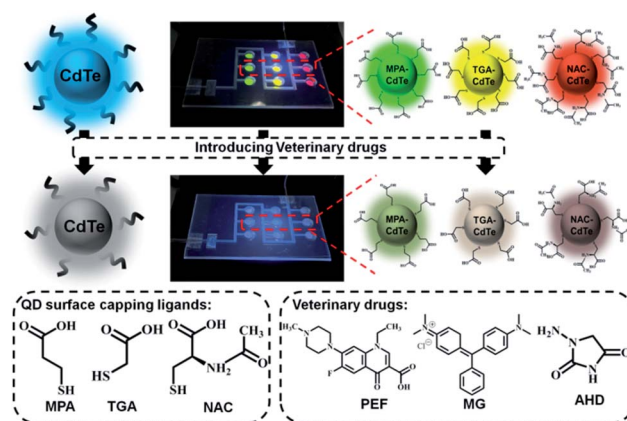
Results and discussion

Three kinds of highly fluorescent multicolor CdTe QDs were successfully prepared *via* an aqueous phase method using 3-mercaptopropionic acid (MPA), thioglycolic acid (TGA) and *N*-acetyl-L-cysteine (NAC) as ligands, respectively, and then we applied them to the field of veterinary drugs detection. This method has the advantages of simple synthesis, easy controllable of experimental conditions and can be used as fluorescent probes without further surface hydrophilic modification, together with providing high-quality CdTe QDs.^{28,29} CdTe QDs can interact with many molecules owing to external carboxyl groups, thus achieving direct application in analytical chemistry. Meanwhile, the carboxyl group is the electron-absorbing group, the surface of QDs has a negative charge, which can be combined with the target molecule with a positive charge through electrostatic interaction, so as to achieve the purpose of detection.^{30,31} Upon the addition of veterinary drugs, the

increase of acidity of the system or the change of the surface energy state of the QDs will lead to fluorescence attenuation or quenching of the QDs. A visual microfluidic fluorescent detection platform was designed for rapid and sensitive detection of different veterinary drugs based on PL sensing ability of multicolor CdTe QDs with multiple capping ligands as fluorescent probes shown in Scheme 1. Combined with the visualized microfluidic QDs platform, this allows simple, fast and intuitive detection of veterinary drugs on samples.

Green-emissive MPA-CdTe QDs, yellow-emissive TGA-CdTe QDs and orange-emissive NAC-CdTe QDs were prepared in the study. As shown in Fig. 1a, the prepared MPA-CdTe, TGA-CdTe and NAC-CdTe QDs emitted bright green, yellow and orange fluorescence under UV (365 nm) irradiation. The photoluminescence (PL) spectra of MPA-CdTe, TGA-CdTe and NAC-CdTe QDs exhibit high fluorescence intensity. At 400 nm excitation wavelength, PL centers were located at 537 nm, 574 nm and 615 nm, respectively (Fig. 1b). Fig. 1c shows the ultraviolet-visible (UV-Vis) absorption spectra of CdTe QDs with different ligands. In the UV-Vis absorption spectra, the optimum absorption peaks for CdTe QDs with different ligands can be observed at 508 nm, 542 nm and 576 nm, respectively. The time-resolved PL decay was tested to explore the PL lifetime and fluorescence decay of CdTe QDs (Fig. 1d). The average PL decay lifetime of MPA-CdTe, TGA-CdTe and NAC-CdTe QDs were fitted by a biexponential decay function as 23.19 ns, 26.24 ns and 34.27 ns, respectively. The long PL decay life lays a foundation for the sensitive detection of QDs in veterinary drugs. In a word, CdTe QDs with good water-solubility, high fluorescence intensity, strong absorption, and long PL decay life were synthesized by using a sulfhydryl water phase method, which is essential for rapid and sensitive detection of veterinary drugs content to meet the needs of practical application.

The microstructures of these CdTe QDs were studied by transmission electron microscopy (TEM). As shown in Fig. 2a–c, the MPA-CdTe, TGA-CdTe and NAC-CdTe QDs are mono-disperse and uniform in size. Clear and identical lattice spacing



Scheme 1 Schematic illustration of a visual microfluidic fluorescent detection platform, based on PL sensing ability of multicolor CdTe QDs with multiple capping ligands, applied for rapid and sensitive detection of different veterinary drugs.

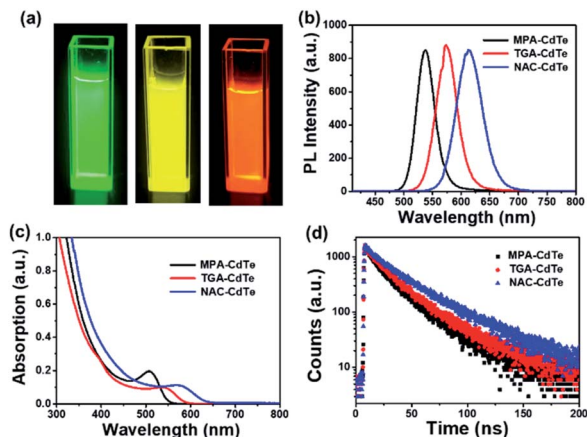


Fig. 1 Optical properties of aqueous solutions of MPA-CdTe QDs, TGA-CdTe QDs and NAC-CdTe QDs: (a) photographs taken under UV (365 nm) irradiation; (b) PL spectra measured under 400 nm excitation; (c) UV-Vis absorption spectra; (d) time-resolved PL decay curves.

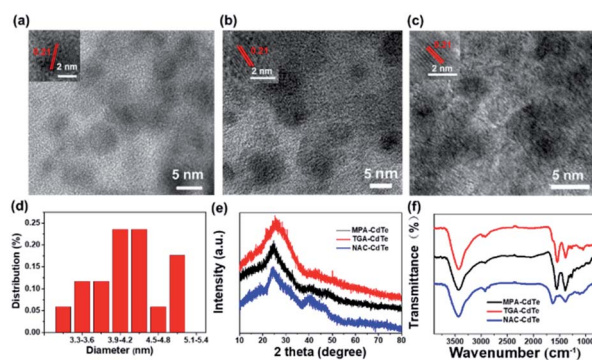


Fig. 2 TEM and HRTEM (inset) images of (a) MPA-CdTe QDs, (b) TGA-CdTe QDs and (c) NAC-CdTe QDs. (d) Size distribution histogram of the MPA-CdTe QDs. (e) XRD patterns of CdTe QDs with different ligands. (f) FT-IR spectra of CdTe QDs with different ligands.

can be seen in high-resolution TEM (HRTEM) observations (inset in Fig. 2a–c), and the lattice stripe with a planar spacing of 0.21 nm matches the (111) plane of CdTe QDs,^{27,32} confirming the good crystallinity of these CdTe QDs. The sizes of the three CdTe QDs are distributed in the regions of 3–6 nm, 3–5 nm and 3–7 nm, with average diameters of 4.2 nm, 5.1 nm and 3.7 nm, respectively (Fig. 2d, S1a and b†). The crystalline structure of these CdTe QDs was further characterized using XRD measurement. As shown in Fig. 2e, the CdTe QDs have a typical zinc blende structure with planes at 111, 220 and 311 and peaks at 24.29°, 40.72° and 46.84°.³³ The good solubility of CdTe QDs in water is attributed to their hydrophilic groups, such as –COOH and –NH₂. As shown in FT-IR spectra (Fig. 2f), 3429 cm^{−1} indicates the O–H vibration, 2968 cm^{−1} and 2922 cm^{−1} represent the presence of C–H. Wave numbers at 1625 cm^{−1}, 1389 cm^{−1} and 1294 cm^{−1} are peaks of characteristic absorption of –COOH. The peaks at 1531 cm^{−1} and 1458 cm^{−1} are attributed to the stretching vibrations of C=O and –NH, respectively. While the characteristic absorption band

of –SH at 2548 cm^{−1} is not seen, which is due to the formation of covalent bonds between Cd²⁺ and –SH.^{34,35} The above results show that the ligand has been successfully covered on the surface of CdTe QDs. All these structural characterization results indicate the successful preparation of well-defined CdTe QDs with different ligands.

CdTe QDs show PL response towards a variety of veterinary drugs and can be used directly as fluorescent probes. The degree of PL quenching correlates with the concentration of the veterinary drug and can be used as an index for veterinary drug residues. Taking the response of CdTe QDs to PEF as an example, we studied the fluorescence changes of CdTe QDs with different ligands to PEF. Firstly, the fresh MPA-CdTe, TGA-CdTe and NAC-CdTe QDs solutions were centrifugally-purified and prepared into aqueous solutions with a concentration of 1 mg mL^{−1}, respectively. Different concentrations of PEF solutions were added into the above series of known concentrations of CdTe QD solutions, and the fluorescence intensity of the mixture changed significantly on the vision. As shown in Fig. 3a–c, under UV (365 nm) irradiation, different fluorescence colours of CdTe QDs with different ligands gradually weakened until quenching with the gradual increase of PEF solution concentration. The mixed detection solution emits weak blue fluorescence under UV (365 nm) irradiation when the concentration of PEF solution is large, which is mainly attributed to the weak blue fluorescence of PEF solution under UV (365 nm) irradiation (Fig. S2†). The weak fluorescence of PEF solution is helpful to visually observe the flow of sample solution in microchannels. So far, there is no unified conclusion about the

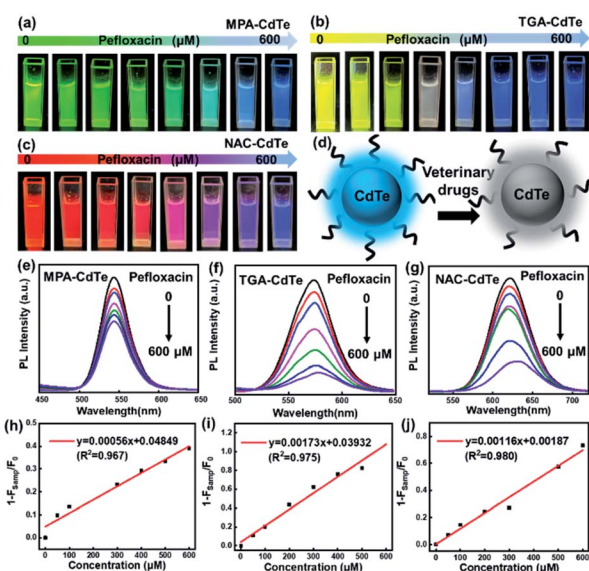


Fig. 3 Photographs of (a) MPA-CdTe QDs, (b) TGA-CdTe QDs and (c) NAC-CdTe QDs with the addition of different concentrations of PEF under UV (365 nm) irradiation. (d) Schematic illustration of CdTe QDs quenched in the presence of veterinary drugs. PL spectra of (e) MPA-CdTe QDs, (f) TGA-CdTe QDs and (g) NAC-CdTe QDs with the addition of different concentrations of PEF. Linear plots of $1 - F_{\text{sample}}/F_0$ of (h) MPA-CdTe QDs, (i) TGA-CdTe QDs and (j) NAC-CdTe QDs versus PEF concentration.



fluorescence quenching mechanism of QDs, which can be summarized as the following hypotheses: energy transfer, electron transfer and surface adsorption of other substances lead to changes in the surface energy state of QDs, resulting in fluorescence quenching of QDs.^{36,37} Studies have shown that the sulfhydryl-containing ligands on the surface of QDs form complexes with Cd^{2+} , reducing the suspended bonds of Te atoms on the surface of QDs. If the acidity of the system increases, the protonation of sulfhydryl groups is enhanced, which leads to the decomposition of the complex and the formation of more suspended bonds on the surface of QDs, reducing the fluorescence intensity of QDs.³⁸ We hypothesized that the acidity of PEF enhanced the protonation of sulfhydryl groups, decomposed the complex and resulted in the formation of more dangling bonds on the surface of CdTe QDs, which reduced the fluorescence intensity of CdTe QDs (Fig. 3d). The variation of fluorescence intensity with the concentration of PEF solution was determined by fluorescence spectrophotometer. PL spectra directly shows the changes in PL intensity of CdTe QDs with MPA, TGA and NAC as ligands at different concentrations of PEF in the range of 0–600 μM , respectively (Fig. 3e–g). As can be seen in the Stern–Volmer plot in Fig. 3h–j, a good linear relationship can be seen between the $1 - F_{\text{samp}}/F_0$ ratio (F_0 and F_{samp} represent the fluorescence intensity of the probe solution before and after the addition of PEF, respectively) and the PEF concentration. The detection limits (LOD) were 7.57 μM , 1.75 μM and 2.90 μM , respectively. The response times were all completed within a few seconds, realizing the sensitive rapid detection of PEF.

In addition, we also studied the fluorescence changes of CdTe QDs with different ligands on veterinary drugs MG and AHD. As shown from the detection results, MG can effectively quench the fluorescence of CdTe QDs. As the concentration of MG increases from 0 μM to 100 μM , the fluorescence intensity of CdTe QDs gradually decreases (Fig. S3a–c†). In Fig. S3d–f†, the ratio of PL intensity between $1 - F_{\text{samp}}$ and F_0 ($1 - F_{\text{samp}}/F_0$) increases linearly from 0 μM to 100 μM with the increase of MG solution concentration. The LODs were $9.20 \times 10^{-4} \mu\text{M}$, $1.16 \times 10^{-4} \mu\text{M}$ and $3.04 \times 10^{-4} \mu\text{M}$, and the correlation coefficients were $R^2 = 0.988$, $R^2 = 0.995$ and $R^2 = 0.983$, respectively. Fig. S4† shows the detection results of AHD. As the concentration of AHD increases, the fluorescence intensity of QDs gradually decreases (Fig. S4a–c†), and the PL intensity ratio of $1 - F_{\text{samp}}$ and F_0 ($1 - F_{\text{samp}}/F_0$) exhibits a linear correlation. The LODs were 2.22 μM , 0.69 μM and 1.89 μM , respectively (Fig. S4d–f†). These three kinds of CdTe QDs with different ligands show different linear relationship in the detection of PEF, MG and AHD and possess the advantages of rapid and sensitive detection, good linear relationship and low LOD. Different linear relationship between $1 - F_{\text{samp}}/F_0$ and CAP concentration could also be observed (Fig. S5†). Therefore, based on the different PL response degree of CdTe QDs with different ligands towards different veterinary drugs, the detection of various veterinary drugs might be available.

Based on the sensitive response of CdTe QDs with different ligands to veterinary drugs, we developed a visual microfluidic detection platform. Fig. 4a and S6† show a microfluidic chip

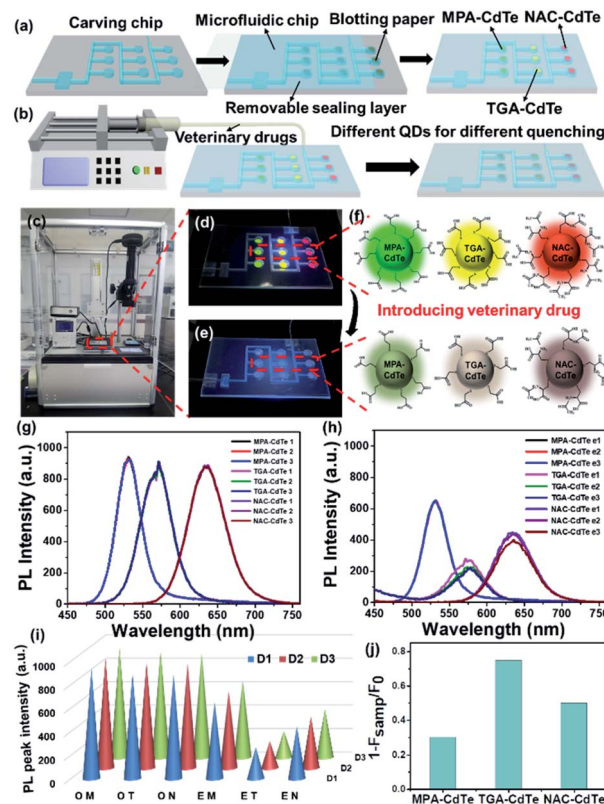


Fig. 4 (a) Schematic illustration of microfluidic detection chip preparation. (b) Schematic illustration of microfluidic detection platform quenching in the presence of various veterinary drugs. Photographs of (c) microfluidic detection platform applied in veterinary drug detection, (d) microfluidic chip before veterinary drug administration and (e) microfluidic chip with veterinary drug in it. (f) Schematic illustration of multicolor CdTe QDs with different ligands responding to veterinary drugs. PL spectra of microfluidic detection platform (g) before and (h) after introducing veterinary drugs. (i) Pattern of PL peak intensity of MPA-CdTe QDs, TGA-CdTe QDs and NAC-CdTe QDs without veterinary drug and with veterinary drug in it. (j) The $1 - F_{\text{samp}}/F_0$ value of different CdTe QDs.

using CdTe QDs of different colors and ligands as fluorescent probes for rapid detection of veterinary drugs. Polymethyl methacrylate (PMMA), which is optically transparent, low-cost and easy to process, was selected as the substrate for microfluidic chips. The microfluidic chip is mainly composed of inlet, serpentine microchannel, detection chamber (circular holes) and buffer pool. The blotting-paper with a diameter of 3 mm is placed in the circular holes and then covered with a detachable sealing layer. CdTe QDs with different ligands were injected separately into circular holes of the detection chamber as fluorescent probes. More details are presented in the Experimental Section. Due to the removable sealing layer, the microfluidic detection chip has the advantages of reusable, cost-saving and beneficial for environmental protection. CdTe QDs with different ligands show different emission peaks and different PL response towards veterinary drugs, and three parallel detection groups could determine the content of veterinary drugs more accurately. As shown in Fig. 4b, the



sample solution containing veterinary drugs flows into the chip through a simple microfluidic device. When the sample solution flows through the serpentine microchannel, it enters the detection chamber, in which different CdTe QDs are quenched to varying degrees. Fig. 4c–e show the response process of veterinary drug (PEF) containing unknown concentration under the microfluidic device. It can be seen that with the entry of the veterinary drug, the CdTe QDs in the detection chamber undergone significant quenching and could be distinguished by the naked eye (Fig. 4d and e). This is mainly due to the enhanced protonation of sulfhydryl groups due to the acidity of PEF, which leads to the decomposition of the complex, resulting in more suspended bonds on the surface of QDs, so that the fluorescence intensity of CdTe QDs is weakened or even quenched (Fig. 4f). It can be seen from the changes of the fluorescence intensity of the initial CdTe QDs (Fig. 4g) and the CdTe QDs after the veterinary drug is injected (Fig. 4h), the concentration of PEF can weaken the CdTe QDs with different ligands to varying degrees. The conical histogram shown in Fig. 4i of the maximum fluorescence peak more intuitively and clearly shows the effect of PEF concentration on the fluorescence of CdTe QDs. The PL intensity ratio of $1 - F_{\text{samp}}/F_0$ (1 – F_{samp}/F_0) of MPA-CdTe, TGA-CdTe and NAC-CdTe QDs are 0.30, 0.75 and 0.50, respectively (Fig. 4j). According to the relationship between the PL intensity and the concentration of veterinary drug solution, the concentration of PEF in the sample is about 420 μM . The parallel three detection groups further increase the accuracy of detection. As shown in Movie S1,† clear visual fluorescence sensing and detection towards veterinary drugs could be achieved *via* this microfluidic detection platform. The visual microfluidic detection platform has the advantages of simplicity, speed and high sensitivity. It has broad application prospects in the real-time quantitative detection of veterinary drug residues. This work promises an effective platform for rapid, sensitive and visual detection of veterinary drug residues, circumventing expensive equipment and complicated operations.

Conclusions

In summary, multicolor CdTe QDs with different ligands were synthesized *via* a sulfhydryl aqueous phase method to show fluorescence sensing toward different veterinary drugs, including PEF, MG, and AHD. Based on the sensitive fluorescence response of CdTe QDs with different ligands to veterinary drugs, we developed a visual fluorescent microfluidic detection platform for veterinary drugs utilizing green MPA-CdTe QDs, yellow TGA-CdTe QDs and red NAC-CdTe QDs as fluorescent probes. With the increase of veterinary drugs concentration, the fluorescence of the probe gradually decreases to a different degree, which can achieve rapid visual sensitive detection of veterinary drugs within a few seconds of ultra-short response time, with good correlation and low LOD. The microfluidic chip with microscale, reusable and three-parallel detectable has the advantages of speed, sensitivity, visualization and increased accuracy, as well as cost saving and environmental protection. Hence, the designed visual fluorescent microfluidic detection

platform offers an attractive way for visual quantitative detection of veterinary drug residues quickly and accurately, which possesses important implications for the development of fluorescent nanosensing in the field of food and environmental safety detection.

Author contributions

Ge Li: methodology, formal analysis, data curation, writing – original draft. Hao Li: investigation, formal analysis, writing – original draft. Jiang Zhai: formal analysis, visualization. Jiazh Huang Guo: investigation, validation. Qing Li: resources, writing – review & editing. Cai-Feng Wang: conceptualization, validation, writing – review & editing, funding acquisition. Su Chen: conceptualization, supervision, funding acquisition. All authors have read and agreed to the published version of the manuscript.

Conflicts of interest

There are no conflicts to declare.

Acknowledgements

This work was supported by the National Key Research and Development Program of China (2018YFC1602800 and 2016YFB0401700), the National Natural Science Foundation of China (21736006 and 21978132), and the Priority Academic Program Development of Jiangsu Higher Education Institutions (PAPD).

Notes and references

- 1 B. M. Bohrer, *Trends Food Sci. Technol.*, 2017, **65**, 103–112.
- 2 A. E. Douglas, *Annu. Rev. Plant Biol.*, 2018, **69**, 637–660.
- 3 Z. Yin, T. Chai, P. Mu, N. Xu, Y. Song, X. Wang, Q. Jia and J. Qiu, *J. Chromatogr. A*, 2016, **1463**, 49–59.
- 4 A. Margalida, G. Bogliani, C. G. R. Bowden, J. A. Donazar, F. Genero, M. Gilbert, W. B. Karesh, R. Kock, J. Lubroth, X. Manteca, V. Naidoo, A. Neimanis, J. A. Sanchez-Zapata, M. A. Taggart, J. Vaarten, L. Yon, T. Kuiken and R. E. Green, *Science*, 2014, **346**, 1296–1298.
- 5 N. Gilbert, *Nature*, 2012, **481**, 125.
- 6 M. Gonzalez Ronquillo and J. C. Angeles Hernandez, *Food Control*, 2017, **72**, 255–267.
- 7 S. Wang, Y. Li, X. Wu, M. Ding, L. Yuan, R. Wang, T. Wen, J. Zhang, L. Chen, X. Zhou and F. Li, *J. Hazard. Mater.*, 2011, **186**, 1513–1519.
- 8 L. Giannetti, A. Giorgi, F. Necci, G. Ferretti, F. Buiarelli and B. Neri, *Anal. Chim. Acta*, 2011, **700**, 11–15.
- 9 C. Nebot, A. Iglesias, R. Barreiro, J. M. Miranda, B. Vázquez, C. M. Franco and A. Cepeda, *Food Control*, 2013, **31**, 102–107.
- 10 F. F. Zhu, J. Peng, Z. Huang, L. M. Hu, G. G. Zhang, D. F. Liu, K. Y. Xing, K. Y. Zhang and W. H. Lai, *Food Chem.*, 2018, **257**, 382–387.
- 11 Y. Zhang, B. Duan, Q. Bao, T. Yang, T. Wei, J. Wang, C. Mao, C. Zhang and M. Yang, *J. Mater. Chem. B*, 2020, **8**, 8607–8613.



- 12 F. Sun, H. Tan, Y. Li, M. De Boevre, H. Zhang, J. Zhou, Y. Li and S. Yang, *J. Hazard. Mater.*, 2021, **401**, 123266.
- 13 J. Alcantara-Duran, D. Moreno-Gonzalez, B. Gilbert-Lopez, A. Molina-Diaz and J. F. Garcia-Reyes, *Food Chem.*, 2018, **245**, 29–38.
- 14 B. Wang, K. Xie and K. Lee, *Foods*, 2021, **10**, 555.
- 15 J. Points, D. Thorburn Burns and M. J. Walker, *Food Control*, 2015, **50**, 92–103.
- 16 Y. Xiao and X. Qian, *Coord. Chem. Rev.*, 2020, **423**, 213513.
- 17 P. K. Mehta, J. Jeon, K. Ryu, S.-H. Park and K.-H. Lee, *J. Hazard. Mater.*, 2022, **427**, 128161.
- 18 S. Mehta and J. Zhang, *Acc. Chem. Res.*, 2021, **54**, 2409–2420.
- 19 S. Wang, B. Li and F. Zhang, *ACS Cent. Sci.*, 2020, **6**, 1302–1316.
- 20 L. Van Hoovels, S. Schouwers, S. Van den Brecht and X. Bossuyt, *Ann. Rheum. Dis.*, 2019, **78**, e48.
- 21 C. Y. Lee, I. Degani, J. Cheong, J. H. Lee, H. J. Choi, J. Cheon and H. Lee, *Biosens. Bioelectron.*, 2021, **178**, 113049.
- 22 S. H. Park, N. Kwon, J. H. Lee, J. Yoon and I. Shin, *Chem. Soc. Rev.*, 2020, **49**, 143–179.
- 23 X. Tao, Y. Peng and J. Liu, *J. Food Drug Anal.*, 2020, **28**, 576–595.
- 24 J. Zhou, Y. Liu, J. Tang and W. Tang, *Mater. Today*, 2017, **20**, 360–376.
- 25 Y. Wu, J. Sun, X. Huang, W. Lai and Y. Xiong, *Trends Food Sci. Technol.*, 2021, **118**, 658–678.
- 26 H. Li, H. G. Ye, R. Cheng, J. Z. Guo, Z. B. Liang, G. Li, Q. Li, C. F. Wang and S. Chen, *J. Lumin.*, 2021, **236**, 118092.
- 27 G. Li, T.-B. Chen, Z. Zhao, L. Ling, Q. Li and S. Chen, *J. Lumin.*, 2020, **228**, 117625.
- 28 K. Ma, T. Fang, J. Bai and H. Guo, *RSC Adv.*, 2013, **3**, 4935–4939.
- 29 C. Hunsur Ravikumar, R. Shwetharani and R. G. Balakrishna, *J. Photochem. Photobiol., B*, 2020, **204**, 111799.
- 30 F. Scholz, L. Ruttinger, T. Heckmann, L. Freund, A. M. Gad, T. Fischer, A. Gutter and H. H. Soffing, *Biosens. Bioelectron.*, 2020, **164**, 112324.
- 31 M. Mahbubur Rahman, D. Liu, N. Siraj Lopa, J.-B. Baek, C.-H. Nam and J.-J. Lee, *Electroanal. Chem.*, 2021, **898**, 115628.
- 32 L. Jing, S. V. Kershaw, T. Kipp, S. Kalytchuk, K. Ding, J. Zeng, M. Jiao, X. Sun, A. Mews, A. L. Rogach and M. Gao, *J. Am. Chem. Soc.*, 2015, **137**, 2073–2084.
- 33 Y. Xu, J. Hao, X. Niu, S. Qi, H. Chen, K. Wang, X. Chen and T. Yi, *Chem. Eng. J.*, 2016, **299**, 201–208.
- 34 F. O. Silva, M. S. Carvalho, R. Mendonça, W. A. A. Macedo, K. Balzuweit, P. Reiss and M. A. Schiavon, *Nanoscale Res. Lett.*, 2012, **7**, 536.
- 35 Q. Wang, T. Fang, P. Liu, B. Deng, X. Min and X. Li, *Inorg. Chem.*, 2012, **51**, 9208–9213.
- 36 T. Senden, R. J. A. van Dijk-Moes and A. Meijerink, *Light: Sci. Appl.*, 2018, **7**, 8.
- 37 M. D. Peterson, S. C. Jensen, D. J. Weinberg and E. A. Weiss, *ACS Nano*, 2014, **8**, 2826–2837.
- 38 J. Hottechamps, T. Noblet, M. Erard and L. Dreesen, *J. Colloid Interface Sci.*, 2021, **594**, 245–253.

